2940
doi:10.1017/S1431927621010254
Microsc. Microanal. 27 (Suppl 1), 2021

High Resolution X-Ray CT Reconstruction of Additively Manufactured Metal Parts using Generative Adversarial Network-based Domain Adaptation in AI-CT

Amir Ziabari[1], Abhishek Dubey[2], Singanallur Venkatakrishnan[1], Curtis Frederick[3], philip Bingham[1], Ryan Dehoff[1] and Vincent Paquit[4]

[1]Oak Ridge National Laboratory, Oak Ridge, Tennessee, United States, [2]Center of Cancer Research, National Cancer Institute, United States, [3]Carl Zeiss Industrial Metrology, United States, [4]Oak Ridge National Laboratory, United States

X-ray computed tomography (XCT) plays a critical role in non-destructive evaluation (NDE) of complex parts in metal additive manufacturing (AM), where characterization of metals in 3D with high spatial resolution is critical for qualification/certification of manufactured parts. However, for metallic objects, beam hardening and metal artifacts pose significant challenges for the analysis of reconstructed images from XCT scanners. This could be further exacerbated due to complex geometry of the part to be scanned as well as the noise and scattering effects in the measurements. Current methods to mitigate the noise and artifacts typically involve very long scan times, making several measurements at localized regions of interests (ROIs) with smaller field of views (FOVs), and development of new algorithm [1-4]. Still, standard approaches produce artifacts for high quality reconstruction of the complex parts being scanned, which make tasks such as detecting pores and defects in the parts very challenging.

We have been developing AI-CT [5], a framework that uses CAD (computer-aided designs) models of the AM parts, along with physics-based parameters to simulate XCT data with noise/artifacts, and leverages a 2.5D convolutional neural network (CNN) to learn to suppress noise/artifacts in the synthetically generated XCT reconstructions. Once the network is trained on the synthetic data, it can be applied to experimental data sets. While promising preliminary results have been shown, for more complex geometries, modeling of the artifacts such as metal artifacts and scattering need more detailed information about the X-ray source, measurement settings and parameters.

In this work, we propose a new framework that extends the capabilities of AI-CT by leveraging generative adversarial networks [6] and domain adaptation [7]. Figs. 1a and b elucidate the process. Starting from a CAD model that is passed through a defect generator to simulate a defective AM part, we model an XCT measurement of the part under study with some default measurement setting, material properties and calibrated physics-based parameters modeling beam hardening and noise. The simulation output along with a real 3D XCT measurement of an AM part is used to train a CycleGAN [6] for performing domain adaptation [7]. In this scenario, the network learns to modify the distribution of the source domain, i.e. simulated XCT volume, to adapt it to the target domain, i.e. the measured XCT volume. Please note that training CycleGAN is unsupervised as the source and target data are unpaired dataset. This trained domain adaptation CycleGAN is then used to generate realistic looking 3D XCT images from the input simulated data. An example of GAN-generated data is shown in Fig. 1b. A pair of GAN-generated XCT volume and the input CAD model (with embedded defects) along with the physics-based beam hardening parameters are used to train the AI-CT, so the network learns to suppress noise and artifacts in the GAN-generated synthetic data to produce high quality reconstruction. The trained network will then be used on real XCT measurement of AM part that manufactured with the same material and are scanned with the same setting.

We designed a proof-of-concept study to evaluate the proposed method. In this study, we took a CAD model (no defect) of an AM part and printed several samples. All these samples were scanned using ZEISS Versa Xardia 620 [8]. Since no ground truth for reconstruction exists, we performed XCT of the samples at two different resolutions of 3.8μm and 11.5μm. The 3.8μm XCT measurement was at a smaller FOV, but ROI

inside the FOV serves as a high-quality ground truth for the lower resolution measurement at the same ROI. Two samples from the batch with low and high porosity were chosen. The low porosity sample was used for domain adaptation using GAN. The other sample was used during testing AI-CT. Examples of results are shown in the Fig. 2. Fig. 2a, shows a qualitative comparison for a slice from the reconstructed volume that is between the standard reconstruction (top) and AI-CT reconstruction (bottom). Figs. 2b-d show a more elaborate example from the ROI. The ROI is measured at ~3X better resolution and every 3 slices in the high resolution (HR) images correspond to one slice from the low resolution (LR) images. Three consecutive slices from the HR volume are shown in Fig. 2b. A slice from the down-sampled volume (HR volume is interpolated (down-sampled) to the same resolution as the LR volume) that corresponds to the three HR slices of Fig. 2b, is shown in Fig. 2c. Fig. 2d is a slice from the output of standard reconstruction algorithm. The output volume is post-processed to remove beam hardening and metal artifacts. Fig. 2e is the corresponding slice from AI-CT's output. The sharpness, high quality and very low noise level of the AI-CT results are evident. In addition, it is clear that AI-CT's high-quality reconstruction has significantly improved the pore detection capability from the LR scan. While these preliminary results are promising, further analyses are being performed to study generalizability of the approach to different measurement settings, scan times and materials.

Acknowledgements.

Research sponsored by the U.S. Department of Energy, Office of Energy Efficiency and Renewable Energy, Advanced Manufacturing Office, under contract DE-AC05-00OR22725 with UT-Battelle, LLC. The US government retains and the publisher, by accepting the article for publication, acknowledges that the US government retains a nonexclusive, paid-up, irrevocable, worldwide license to publish or reproduce the published form of this manuscript, or allow others to do so, for US government purposes. DOE will provide public access to these results of federally sponsored research in accordance with the DOE Public Access Plan (http://energy.gov/downloads/doe-public-access-plan). A.D and S.V were supported by AI-initiative LDRD Program at ORNL.

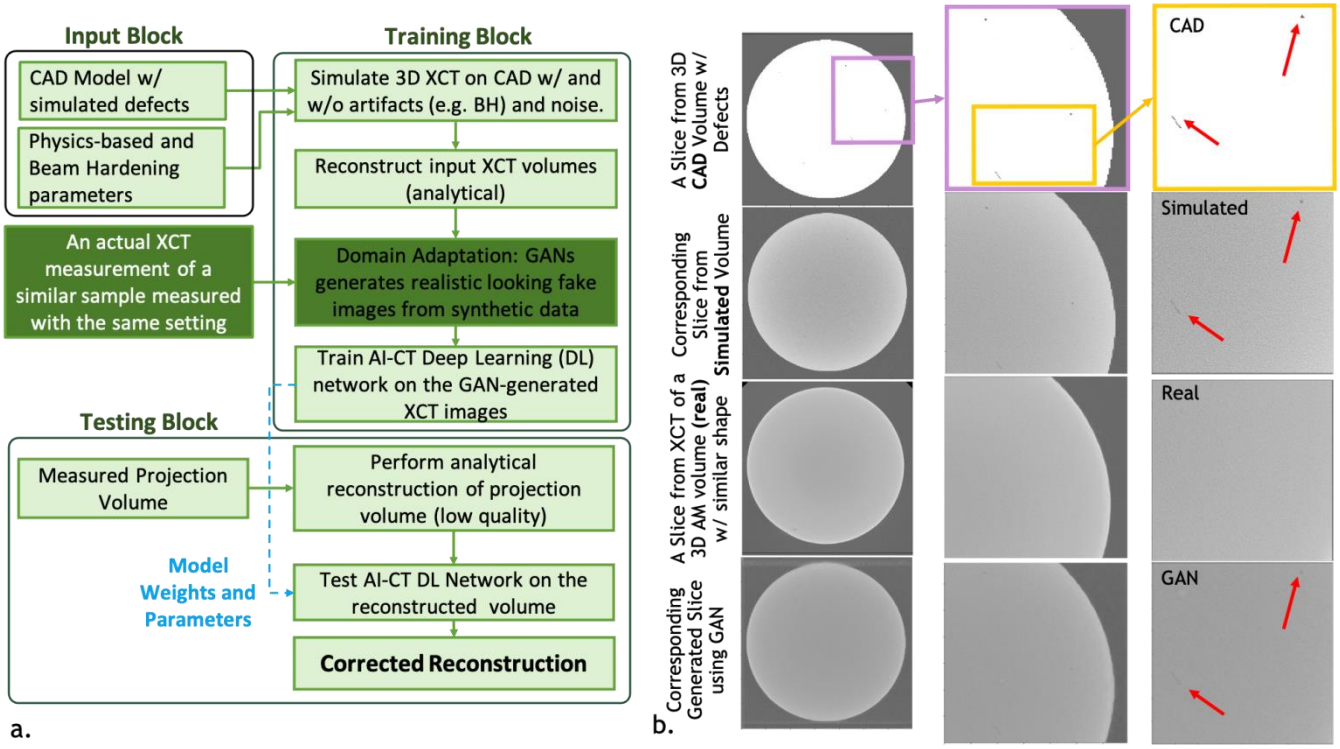

Figure 1. Figure 1. a) AI-CT algorithm with GAN-based Domain Adaptation. b) A slice from different volumes (CAD with embedded defects, simulation, measurement and GAN-generated data) that are used in the algorithm.

https://doi.org/10.1017/S1431927621010254 Published online by Cambridge University Press

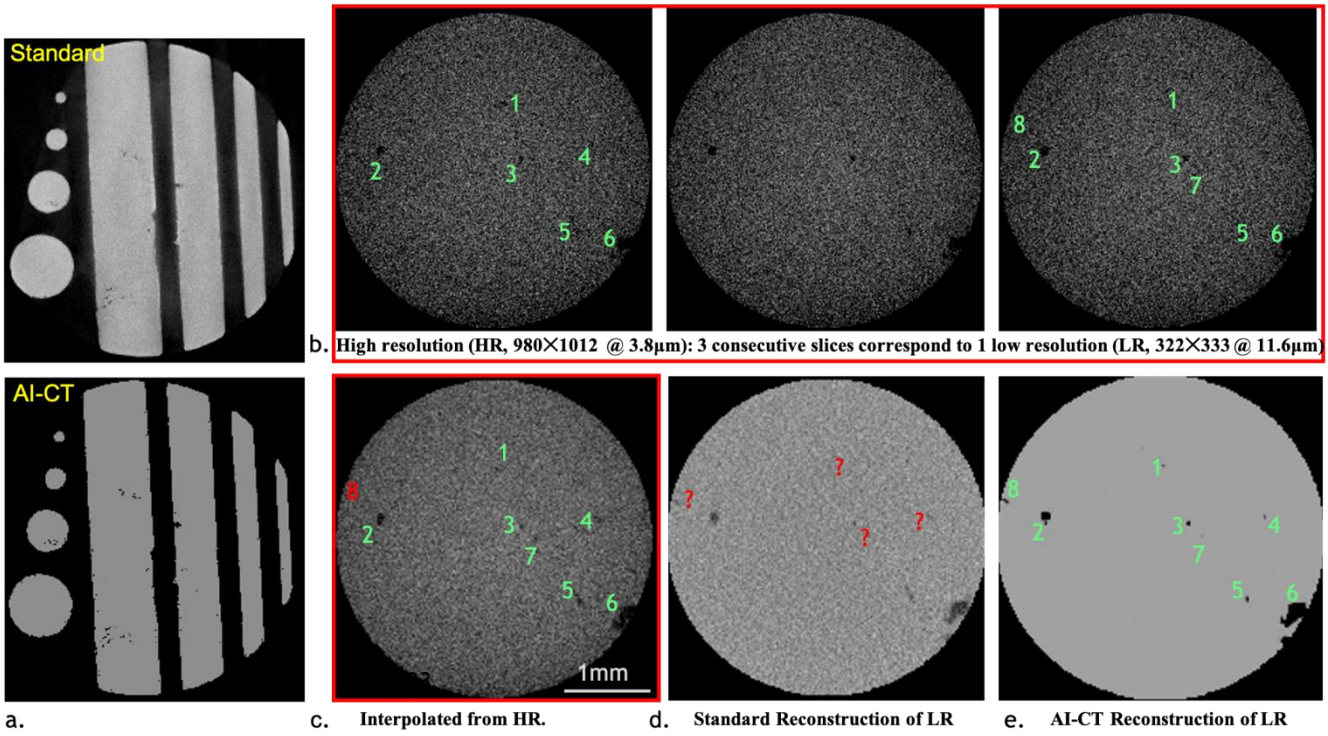

Figure 2. Figure 2. a) a qualitative comparison between AI-CT and standard reconstruction for a single slice from the 3D volume. b) Three consecutive slices from the 3D volume at 3.8μm resolution (HR data). c) Corresponding downsampled slice from HR data. d) Standard reconstruction from a measurement at 11.6μm resolution (LR data). e) AI-CT output based on LR data.

References

[1] P.Jin, C. A. Bouman, and K. D. Sauer, "A Model-Based Image Reconstruction Algorithm With Simultaneous Beam Hardening Correction for X-Ray CT," *IEEE Trans. Comput. Imaging*, vol. 1, no. 3, pp. 200–216, 2015.

[2] V. Ruth, D. Kolditz, C. Steiding, and W. A. Kalender, "Metal artifact reduction in X-ray computed tomography using computer-aided design data of implants as prior information," *Invest. Radiol.*, vol. 52, no. 6, pp. 349–359, 2017.

[3] E. Van de Casteele, D. Van Dyck, J. Sijbers, and E. Raman, "An energy-based beam hardening model in tomography," *Phys. Med. Biol.*, vol. 47, no. 23, pp. 4181–4190, 2002.

[4] S. Xu and H. Dang, "Deep residual learning enabled metal artifact reduction in CT," in *SPIE Medical Imaging*, 2018, no. 10573, p. 132.

[5] A.Ziabari*et al.*, "Beam hardening artifact reduction in x-ray ct reconstruction of 3d printed metal parts leveraging deep learning and cad models,"inProceedings of the ASME 2020 International Mechanical Engineering Congress and Exposition(IMECE), 2020, p. V02BT02A043.

[6] J. Y. Zhu, T. Park, P. Isola, and A. A. Efros, "Unpaired Image-to-Image Translation Using Cycle-Consistent Adversarial Networks," *Proc. IEEE Int. Conf. Comput. Vis.*, vol. 2017-Octob, pp. 2242–2251, 2017.

[7] G. Wilson and D. J. Cook, "A Survey of Unsupervised Deep Domain Adaptation," *ACM Trans. Intell. Syst. Technol.*, vol. 11, no. 5, pp. 1–46, 2020.

[8] "ZEISS Versa Xardia 620." [Online]. Available: https://www.zeiss.com/microscopy/us/products/x-ray-microscopy/zeiss-xradia-610-and-620-versa.html.

https://doi.org/10.1017/S1431927621010254 Published online by Cambridge University Press